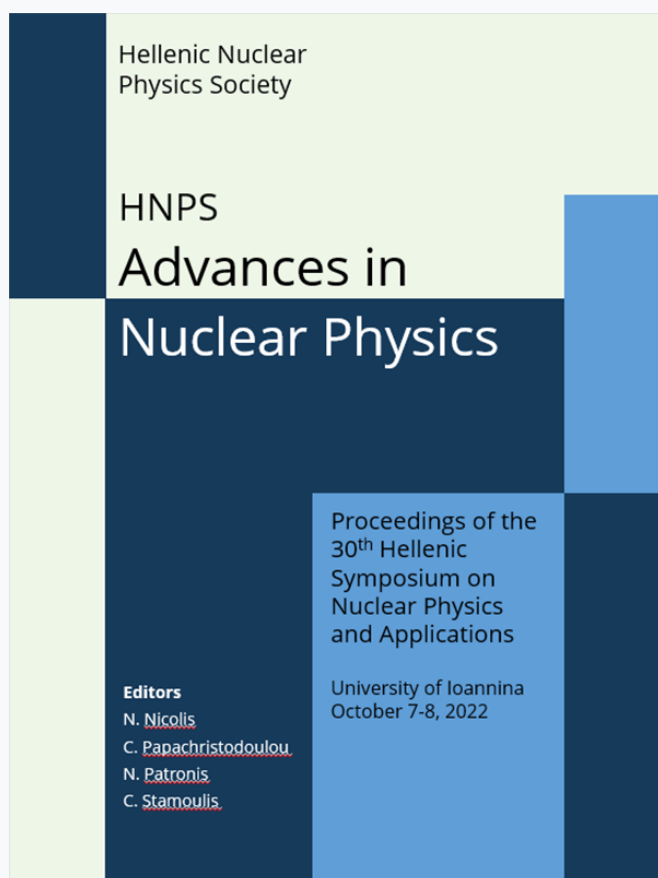


HNPS Advances in Nuclear Physics

Vol 29 (2023)

HNPS2022



Momentum Distribution Studies of Projectile Fragments from Peripheral Collisions Below the Fermi Energy

Olga Fasoula, George A. Souliotis, Stergios Koulouris, Konstantina Palli, Martin Veselsky, Sherry J. Jenello, Aldo Bonasera

doi: [10.12681/hnpsanp.5089](https://doi.org/10.12681/hnpsanp.5089)

Copyright © 2023, Olga Fasoula, George A. Souliotis, Stergios Koulouris, Konstantina Palli, Martin Veselsky, Sherry J. Jenello, Aldo Bonasera



This work is licensed under a [Creative Commons Attribution-NonCommercial-NoDerivatives 4.0](https://creativecommons.org/licenses/by-nc-nd/4.0/).

To cite this article:

Fasoula, O., Souliotis, G. A., Koulouris, S., Palli, K., Veselsky, M., Jenello, S. J., & Bonasera, A. (2023). Momentum Distribution Studies of Projectile Fragments from Peripheral Collisions Below the Fermi Energy. *HNPS Advances in Nuclear Physics*, 29, 38–44. <https://doi.org/10.12681/hnpsanp.5089>

Momentum Distribution Studies of Projectile Fragments from Peripheral Collisions Below the Fermi Energy

O. Fasoula^{1,*}, G. A. Souliotis¹, S. Koulouris¹, K. Palli¹, M. Veselsky²,
S. J. Yennello³, A. Bonasera³

¹ *Laboratory of Physical Chemistry, Department of Chemistry, National and Kapodistrian University of Athens, Greece*

² *Institute of Experimental and Applied Physics, Czech Technical University, Prague, Czech Republic*

³ *Cyclotron Institute, Texas A&M University, College Station, Texas, USA*

Abstract This paper presents our recent studies of multinucleon transfer in peripheral collisions in reactions below the Fermi regime. Our current focus is on the study of the mass, angular and momentum distributions of the projectile-like fragments from the reaction of an ⁸⁶Kr beam at 15 MeV/nucleon with a target of ⁶⁴Ni. The study of momentum distributions is a new direction of our endeavors. Experimental data from our previous work with the MARS spectrometer at the Cyclotron Institute of Texas A&M University were compared with model calculations. The dynamical stage of the reaction is described with either the Deep-Inelastic Transfer Model (DIT) or with the microscopic Constrained Molecular Dynamics model (CoMD). The de-excitation of the hot projectile-like fragments is performed with the GEMINI model. The momentum distributions are characterized by a quasi-elastic peak and a deep-inelastic peak. Two-body kinematics was employed to extract the total excitation energies of these regions. The comparison between these models and the experimental data is expected to provide useful insight toward understanding the complexities of the reactions in this energy regime.

Keywords multinucleon transfer, momentum distribution, Fermi energy regime, neutron rich isotopes, multiple charge exchange

INTRODUCTION

The exploration of rare isotopes and the reaction mechanism(s) that produce them are among the fundamental interests of modern nuclear physics [1-4]. Reaching these nuclei provides us with valuable information on r-process nucleosynthesis which is responsible for the production of a large amount of the heavier elements [5-7]. Apart from fragmentation [8] and spallation [9], multinucleon transfer reactions offer the means to produce these nuclei. Our group specifically focuses on the study of these reactions in the Fermi energy regime (15-35 MeV/nucleon) [10-18]. In this work we present the study of a reaction with a ⁸⁶Kr beam at 15 MeV/nucleon with a target of ⁶⁴Ni. The experimental data were obtained with the Momentum Achromat Recoil Separator (MARS) at the Cyclotron Institute at Texas A&M University in previous work of our group [12]. As part of the systematic analysis of the data, the momentum distributions were extracted from the original data [14]. We also performed calculations with two models, and we present a comparison of the calculations with the mass, angular and momentum distributions of the experimental data.

THEORETICAL MODELS

The theoretical models used in this work are based on a two-stage approach. Excited projectile-like fragments and excited target-like fragments are produced after the dynamical part of the collisions between the projectile and the target. This stage of the reactions was simulated either with the Deep Inelastic Transfer model (DIT) or the Constrained Molecular Dynamics model (CoMD). We focus

* Corresponding author: olgafas@chem.uoa.gr

mainly on the projectile-like fragments. After this first dynamical stage, the de-excitation of the hot projectile-like fragments was performed by the GEMINI model.

The DIT model [19] is a phenomenological model used in peripheral collisions and it simulates the stochastic exchange of nucleons via a ‘window’ between the projectile and the target. The CoMD model [20-22] is a microscopic, semiclassical model based on quantum dynamics. The nucleons are considered as Gaussian wave packets, and the interactions take place via a phenomenological effective potential. The fermionic nature of the system is introduced by the Pauli principle through proper restrictions in the phase space. In both models, successive events are simulated through Monte Carlo implementation. The GEMINI [23, 24] model, used for de-excitation of the primary nuclei after the interaction, is a binary de-excitation model.

COMPARISON OF DATA AND CALCULATIONS

In this section, we present mass, angular and momentum distributions of projectile-like fragments from the reaction 15 MeV/nucleon $^{86}\text{Kr} + ^{64}\text{Ni}$ along with model calculations.

Mass distributions: 15 MeV/nucleon $^{86}\text{Kr} + ^{64}\text{Ni}$

In Fig. 1, we present the mass distributions of projectile-like fragments within the atomic number region of $Z=30-37$ from the reaction 15 MeV/nucleon $^{86}\text{Kr} + ^{64}\text{Ni}$ along with model calculations. Black dots are the experimental data [12], green lines are DIT/GEMINI calculations and red lines are CoMD/GEMINI calculations. Solid lines represent the final fragments after the de-excitation and dashed lines represent the primary hot-projectile-like fragments. The fragments after the vertical blue dashed line come from neutron pickup.

It is noteworthy that for masses near the projectile ($Z=34-36$), very neutron rich isotopes are produced. For example, for Kr we observe pickup up to 7 neutrons and for Br up to 6 neutrons.

Angular and Momentum Distribution Studies

A new part of our systematic analysis of these reactions is the study of momentum distributions in tandem with angular distributions. In Fig. 2 we present the angular (left) and momentum (right) distributions of several projectile-like fragments on the same reaction, specifically the neutron pickup channels (+1n to +4n).

As for the angular distributions, each panel represents a specific isotope and the corresponding scattering angle and angular differential cross sections. There are two experimental points, one for each setting of the MARS spectrometer at 4° ($2.2^\circ-5.8^\circ$) and 7° ($5.6^\circ-9.2^\circ$) both with an angular width of 3.6° [12]. For this system, the grazing angle is $\theta_{gr}=6^\circ$, so we expect that the 4° data setting is the appropriate one to accept quasi-elastic products.

As for the momentum distributions, each panel represents a specific isotope and the corresponding momentum per nucleon and differential cross sections. We note that the momentum per nucleon (P/A) expresses the velocity of the ejectiles and gives us an indication of the extent of the dissipation. The experimental data have some interesting characteristics. Generally, there are two main regions. One region in higher P/A that corresponds to quasi-elastic events with low total kinetic energy loss and a region in lower P/A that corresponds to more dissipative events with larger total kinetic energy loss. Also, we note that the deeps in the experimental data are due to gates on the elastically scattered ^{86}Kr projectiles in the most intense charged states. Finally, the numbers on top of the peaks are the total excitation energies of the system (projectile-target) in MeV which were extracted through binary kinematics calculations.

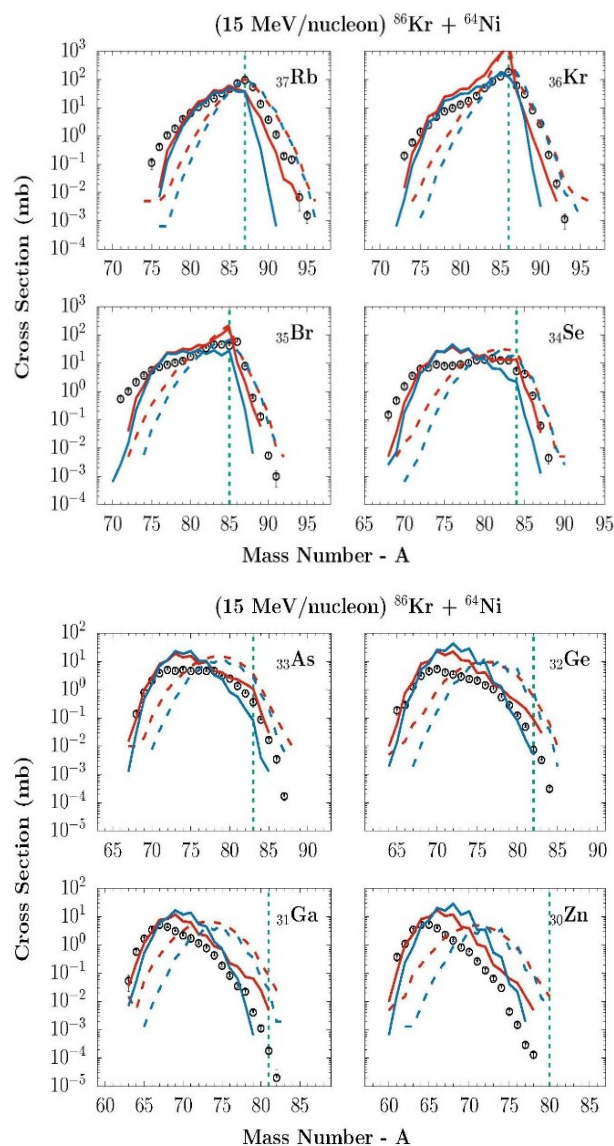


Figure 1. Comparison of calculations with experimental mass distributions of projectile-like fragments from the reaction of 15 MeV/nucleon $^{86}\text{Kr} + ^{64}\text{Ni}$. Solid red lines: COMD/GEM for the de-excited projectile-like fragments. Dashed red lines: COMD/GEM for the primary projectile-like fragments. Solid blue lines: DIT/GEM for the de-excited projectile-like fragments. Dashed blue lines: DIT/GEM for the primary projectile-like fragments. Vertical green dashed lines indicate the beginning of neutron pickup.

Neutron Pickup: Angular and Momentum Distributions 15 MeV/nucleon $^{86}\text{Kr} + ^{64}\text{Ni}$

In Fig. 2 we present angular and momentum distributions this time on neutron pickup channels (+1n to +4n).

The DIT/GEMINI calculations seem to follow the data, especially in the addition of one or two neutrons (^{87}Kr and ^{88}Kr) but not so adequately for the addition of three and four neutrons (^{87}Kr and ^{88}Kr). The CoMD/GEMINI calculations seem to follow the descending tendency of the data but appear to yield lower values than the DIT/GEMINI calculations.

Both DIT/GEMINI and CoMD/GEMINI calculations seem to follow the ascending pattern of the data but there are discrepancies with the description of the different peaks of the distributions, with a steadily ascending shape as P/A increases. These features are currently under investigation.

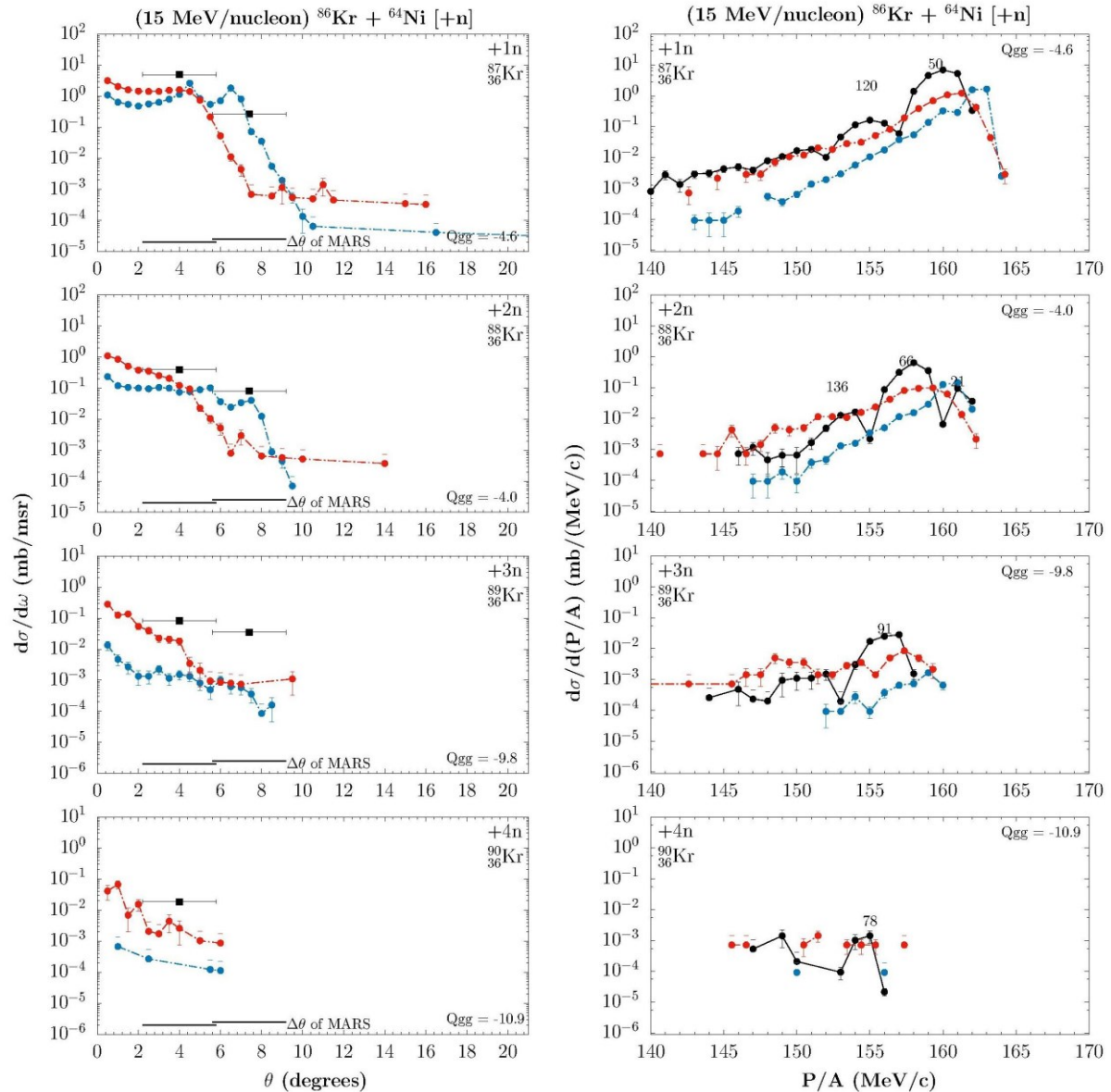


Figure 2. Comparison of calculations with experimental angular (left) and momentum (right) distributions of projectile-like fragments from the reaction of 15 MeV/nucleon $^{86}\text{Kr} + ^{64}\text{Ni}$. Neutron pickup channels. Q_{gg} : Q -values of corresponding channels. Black symbols: Exp. data. Red symbols: COMD/GEM calculations. Blue Symbols: DIT/GEM calculations.

Proton Removal: Angular and Momentum Distributions 15 MeV/nucleon $^{86}\text{Kr} + ^{64}\text{Ni}$

In Fig. 3 we follow the same pattern of figures with angular and momentum distributions this time on proton removal channels (-1p to -4p).

Once more, on the angular distributions the DIT/GEMINI calculations have an overall agreement with the data particularly on the 4° data and on the removal of one to three protons (^{85}Br , ^{84}Se , ^{83}As). The CoMD/GEMINI calculations yield lower values than the DIT/GEMINI calculations but again follow the general trend of the data.

On the momentum distributions both calculations show similar trends again with a steadily ascending shape as P/A increases.

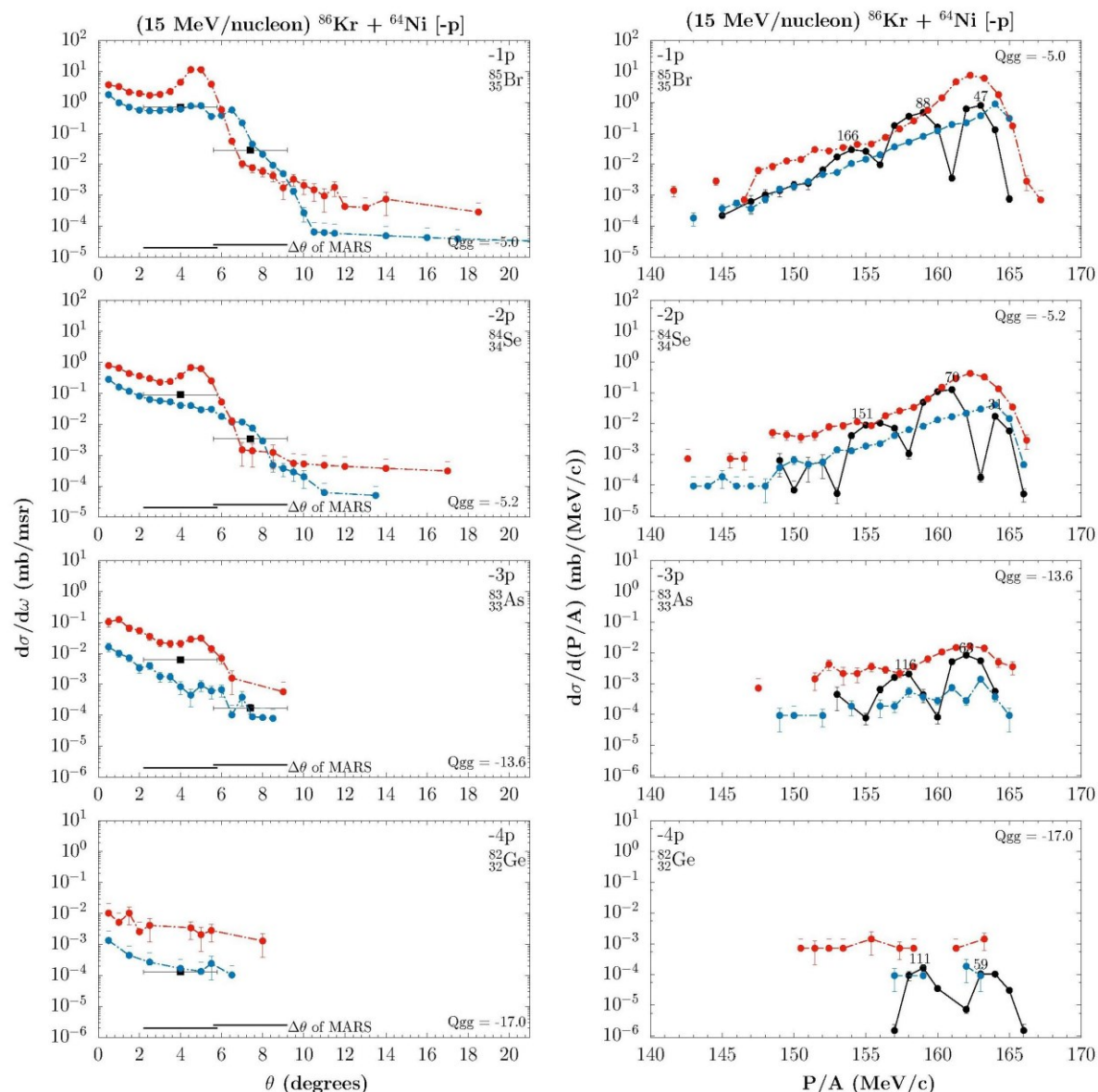


Figure 3. Comparison of calculations with experimental angular (left) and momentum (right) distributions of projectile-like fragments from the reaction of 15 MeV/nucleon $^{86}\text{Kr} + ^{64}\text{Ni}$. Proton removal channels. Q_{gg} : Q -values of corresponding channels. Black symbols: Exp. Data. Red symbols: COMD/GEM calculations. Blue Symbols: DIT/GEM calculations.

Multiple Charge Exchange: Angular and Momentum Distributions 15 MeV/nucleon $^{86}\text{Kr} + ^{64}\text{Ni}$

Finally, in Fig. 4 we present angular and momentum distributions on multiple charge exchange channels ($-1p+1n$ to $-3p+3n$).

Both in angular and momentum distributions there are no calculations on the channel of the removal of three protons and addition of three neutrons (^{86}As). This emphasizes the need of extensive statistics in order to cover experimental data with extremely low cross sections. We are currently working on calculations to reach these regions.

This time, on both the angular and the momentum distributions the calculations have comparable shapes and follow the same patterns as in the two previous channels.

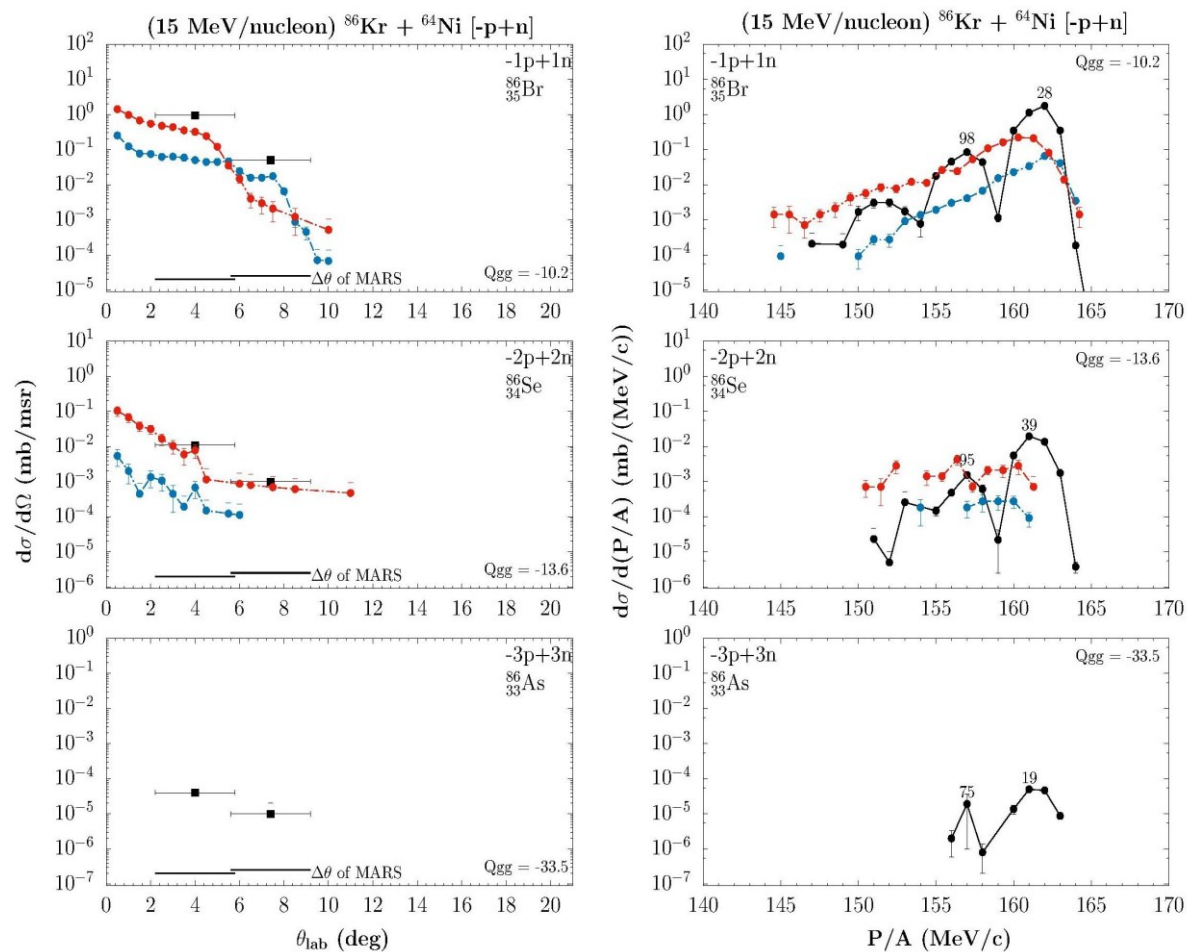


Figure 4. Comparison of calculations with experimental angular (left) and momentum (right) distributions of projectile-like fragments from the reaction of 15 MeV/nucleon $^{86}\text{Kr} + ^{64}\text{Ni}$. Multiple charge exchange channels. Q_{gg} : Q -values of corresponding channels. Black symbols: Exp. Data. Red symbols: COMD/GEM calculations. Blue Symbols: DIT/GEM calculations.

CONCLUSIONS - DISCUSSION

In this work, we presented a systematic study of mass, angular and momentum distributions on the reaction with an ^{86}Kr beam at 15 MeV/nucleon with a target of ^{64}Ni . The mass distributions and the recently extracted momentum distributions of the projectile-like fragments indicate the production of very neutron rich isotopes. We also performed calculations with the DIT and CoMD models with an overall good agreement with the experimental data and the presence of some discrepancies.

Concerning our future steps, we plan to continue the systematic analysis of various distributions of experimental data and explore the different parameters of DIT and CoMD models in order to describe the data more accurately. Moreover, we will perform kinematic analysis on the momentum distributions leading to a reconstruction of the quasi-projectile. Finally, we plan to employ direct reactions codes such as Fresco and Ptolemy to describe the quasi-elastic part of the observed distributions. These efforts constitute an important step toward understanding the reaction mechanisms responsible for the production of exotic neutron rich nuclei in the Fermi energy regime.

References

- [1] F. Nowacki, A. Obertelli, A. Poves, Prog. Part. Nucl. Phys. 120, 103866 (2021)
- [2] J. J. Cowan et al., Rev. Mod. Phys. 93, 015002 (2021)

- [3] C. J. Horowitz et al., *J. Phys. G: Nucl. Part. Phys.* 46, 083001 (2019)
- [4] Q. Z. Chai, Y. Qiang, J. C. Pei, *Phys. Rev. C* 105, 034315 (2022)
- [5] M. Arnould, S. Goriely, *Prog. Part. Nucl. Phys.* 112, 103766 (2020)
- [6] J. Erler, N. Birge, M. Kortelainen et al., *Nature* 486, 509 (2011)
- [7] J. J. Cowan, F.K. Thielemann, *Physics Today*, 57(10), 47 (2004)
- [8] Y. Blumenfeld, T. Nilsson and P. Van Duppen, *Phys. Scr. T152* 014023 (2013)
- [9] A. Kelic, M. V. Ricciardi, K. -H. Schmidt, *BgNS Transactions* 13, 98 (2009)
- [10] G. A. Souliotis et al., *Phys. Lett. B* 543, 163 (2002)
- [11] G. A. Souliotis et al., *Phys. Rev. Lett.* 91, 022701 (2003)
- [12] G. A. Souliotis et al., *Phys. Rev. C* 84, 064607 (2011)
- [13] O. Fasoula, G. A. Souliotis et al., arXiv:2103.10688
- [14] O. Fasoula, G. A. Souliotis et al., *HNPS Adv. Nucl. Phys.* 28, 47 (2022)
- [15] S. Koulouris. Fasoula, G. A. Souliotis et al., *HNPS Adv. Nucl. Phys.* 28, 42 (2022)
- [16] K. Palli, G. A. Souliotis et al., *HNPS Adv. Nucl. Phys.* 28, 286 (2022)
- [17] K. Palli, G. A. Souliotis et al., *EPJ Web of Conferences* 252, 07002 (2021)
- [18] S. Koulouris, G.A. Souliotis et al., *EPJ Web of Conferences* 252, 07005 (2021)
- [19] L. Tassan-Got, C. Stephan, *Nucl. Phys. A* 524, 121 (1991)
- [20] M. Papa, T. Maruyama, A. Bonasera, *Phys. Rev. C* 64, 024612 (2001)
- [21] M. Papa, G. Giuliani, A. Bonasera, *J. Comput. Phys.* 208, 403 (2005)
- [22] T. Depastas, G. A. Souliotis, et al., *EPJ Web of Conferences* 252, 07003 (2021)
- [23] R. J. Charity et al., *Nucl. Phys. A* 483, 371 (1988)
- [24] R. J. Charity, *Phys. Rev. C* 58, 1073 (1998)